

ON THE USE OF THE STIELTJES INTEGRALS IN THE SOLUTION OF THE INVERSE PROBLEMS FOR AEROSOL LIGHT SCATTERING

V.V. Veretennikov and E.P. Yausheva

*Institute of Atmospheric Optics,
Siberian Branch of the Russian Academy of Sciences, Tomsk
Received October 15, 1991*

A new numerical scheme has been proposed for reconstructing the microstructure and the refractive index of aerosol from the angular measurements of scattering matrix components. The inversion method is based on representation of the polydisperse characteristics of scattering in the form of the Stieltjes integrals and minimization of the discrepancy functional on a set of monotone bounded functions. Such an approach impose no restrictions on the smoothness of aerosol microstructural distributions. Moreover, it is not necessary to solve the problem on choosing a regularization parameter. The results of numerical modeling of the inverse problem are given as well as an example of the interpretation from the data of field experiments.

1. Introduction. In the course of solving the inverse problems for aerosol light scattering, the Reimann integral representation is usually employed to describe polydisperse optical characteristics. The aerosol particle size distribution in this case is characterized by the function $n(r)$ so that the value $n(r)dr$ determines the number of particles whose radii lie in the interval $[r, r + dr]$. Since real aerosol distributions are discrete, such a representation is, to a certain extent, mathematical idealization and can be acceptable if the particles are distributed sufficiently dense on each small interval $[r, r + dr]$. It is clear that these arguments are of qualitative nature and pertain not only to the size distribution of the particle number density $n(r)$ but also to the associated distribution functions of particles over size of the geometric cross section $s(r)$ and over the volume $v(r)$ which are also employed for the description of the aerosol microstructure. The limitation on the application of this description of microstructure with such differential distributions is manifested in the solution of inverse problems, during the regularization of which a class of admissible solutions gets narrower due to the requirements of continuity, smoothness, etc.

From this point of view, many restrictions can be overcome if we make use of an alternative representation of polydisperse characteristics of scattering in the form of the Reimann–Stieltjes integrals. Such a representation of spectral optical characteristics was discussed elsewhere.¹ The present paper deals with one of the possible calculational schemes for simultaneous reconstruction of the microstructure and the refractive index of aerosol by inverting the angular polarization characteristics of scattering represented in the form of the Stieltjes integrals.

2. Formulation of the problem and scheme for inversion. For definiteness, below we are concerned with the distribution functions of particles over size of geometric cross section. Let us denote by $S(r)$ the function prescribed on the interval $[0, R]$. This function determines the total geometric cross section of particles with radius smaller than or equal to r . We examine now some properties of the function $S(r)$ determining the class of functions Ω to which it belongs. This function is positive, monotonically nondecreasing, uniformly bounded on the interval $[0, R]$ and continuous from the left. It is well known that any monotone function can be represented as a sum of a continuous monotone function and a jump function. Therefore, we can write the expansion

$$S(r) = \tilde{S}(r) + \sum_{r_k < r} \sigma_k, \quad (1)$$

where $\tilde{S}(r)$ is the continuous monotone function with the derivative $d\tilde{S}/dr = s(r)$, and the second term prescribes a jump function at discontinuity points r_k . In the problem under study the jump function determines the existence of a monodisperse fraction of particles with radii r_k and total cross section σ_k .

Using the distribution function $S(r)$ for describing the disperse composition of aerosol particles, it is possible to represent any optical characteristics, e.g., the scattering phase function $\mu(\theta)$ in the form of the Stieltjes integral

$$\mu(\theta) = \int_0^R K(\theta, r) dS(r), \quad (2)$$

in which the kernel $K(\theta, r) = (i_1 + i_2)/(2\pi x^2)$ and $x = 2\pi r/\lambda$, where i_1 and i_2 are the functions of the dimensionless intensity² and λ is the wavelength. By virtue of expansion (1), integral (2) can be written in the form

$$\int_0^R K(\theta, r) dS(r) = \sum_k K(\theta, r_k) \sigma_k + \int_0^R K(\theta, r) s(r) dr. \quad (3)$$

To determine the function $S(r)$ from Eq. (2), it is convenient to integrate it preliminary by parts:

$$\int_0^R K(\theta, r) dS(r) = K(\theta, r) S(r) \Big|_0^R - \int_0^R S(r) dK(\theta, r). \quad (4)$$

which leads to the equation for the function $S(r)$

$$K(\theta, r) S(r) - \int_0^R \frac{\partial K(\theta, r)}{\partial r} S(r) dr = \mu(\theta), \quad (5)$$

or to the equation

$$\int_0^R \frac{\partial K(\theta, r)}{\partial r} S_{\downarrow}(r) dr = \mu(\theta) \quad (6)$$

for the function $S_{\downarrow}(r) = S(R) - S(r)$. Equations (5) and (6) have a general form of the equation of the first type

$$QS = \mu. \quad (7)$$

It follows from the properties of the function $S(r)$ that its variations are bounded. Then, following the Helly theorem,³ there exists a sequence of functions in Ω which converges at every point to a certain function from Ω . The convergence at every point and uniform boundedness imply the convergence in $L_p[0, R]$, where $p > 1$, i.e., the set Ω is a compact in $L_p[0, R]$. Now the developed theory has been created and the effective numerical algorithms have been constructed for solving the ill-posed inverse problems on compact sets.⁴ Since the rigorous solution $S_0(r)$ belongs to the compact set Ω , it is sufficient to minimize the discrepancy functional

$$F^2 = \|QS - \mu\|^2 \quad (8)$$

in order to construct a stable approximate solution of Eq. (7) on the set Ω (see Ref. 4). Any function $S_{\delta}(r) \in \Omega$ for which the functional $F^2 \leq \delta^2$, where δ^2 characterizes an error in the input data, can be taken as an approximate solution of Eq. (7). In this case the convergence $S_{\delta}(r) \rightarrow S_0(r)$ takes place in space $L_p[0, R]$ for $p > 1$. Note some other important properties of the approximate solution $S_{\delta}(r)$ found in Ref. 4. If $S_0(r)$ is known to be a continuous function which corresponds to the absence of the second term in Eq. (1), then $S_{\delta}(r)$ uniformly converges to $S_0(r)$. The approximate solution $S_{\delta}(r)$ in this case can be a discontinuous monotone function. Finally, if $S_0(r)$ is a piecewise-continuous function, then $S_{\delta}(r) \rightarrow S_0(r)$ uniformly on each closed segment which does not include the discontinuity points of the rigorous solution $S_0(r)$.

The following differences can be noted in the aforementioned approach to the problem of determining the aerosol microstructure from the optical characteristics of scattering and the methods employing regularizing algorithms which implement minimization of the smoothing functional.⁵ Transition to the integral representation of the microstructure of aerosol distributions enables one to extend substantially the class of correctness when solving the inverse problems. The smoothing functional method is mainly tailored to the problems of reconstructing continuous smooth aerosol distributions $s(r)$. If the distributions $s(r)$ are discontinuous and have no required smoothness, the transition to the representation of the dispersion composition with the integral distributions $S(r)$ is expedient. In this case to describe discontinuities in distributions $s(r)$ it is sufficient to employ a piecewise-linear approximation for the function $S(r)$. Moreover, if we assume the existence of discontinuities in the function $S(r)$, then it becomes possible to treat situations describing the presence of monodisperse aerosol fractions which correspond to the δ -singularities in the distributions $s(r)$.

The other important advantages of solution of inverse problem (7) on the compact Ω , is the possibility of estimating the error of the approximate solution based on the information about the value of the error in the initial data.⁴

Characterization of the ensembles of aerosol particles with the integral distributions $S(r)$ is less applicable than the other methods for describing the dispersion composition of aerosol. Accordingly, using representation (4) it is possible to transfer to more usual and obvious microstructural parameters such as a particle number density, a volume fill factor, and moments of different order, including a mean value, a half-width, etc. For example, the volume fill factor V and the particle radius r_s , averaged over the distribution $s(r)$ are expressed in terms of the function $S(r)$ based on the formulas

$$V = a \left[RS(R) - \int_0^R S(r) dr \right],$$

$$r_s = V/[aS(R)], \quad a = 4/3.$$

3. Reconstruction of the refractive index. The method for estimating the refractive index $m - i\kappa$ is analogous to that described elsewhere⁶ for differential distributions $s(r)$, but, in contrast to the latter, it does not require the determination of the regularization parameter for the inverse problem with an approximately assigned operator. Now we will briefly dwell on estimating the refractive index from the measurements of two optical characteristics, e.g., the polarization scattering phase functions $\mu_i = Q_i S$ ($i = 1, 2$). For simplicity, we will discuss the reconstruction of only one parameter, i.e., a real part of the refractive index m .

Let m_0 be an exact value of the real part of the refractive index which belongs to a certain *a priori* assigned region P . Then for arbitrary $m \in P$ the solution S reconstructed by minimizing functional (8) for one of the polarization scattering phase functions, e.g., μ_1 , is also dependent on the chosen value of the parameters m . The method for estimating the parameter m is based on minimizing in the region P the discrepancy in the measured second characteristic μ_2 and the scattering phase function μ_2 calculated from the microstructure $S_1 = S(r, m)$ which has been reconstructed by inverting μ_1

$$F_{12}^2(m) = \|Q_2(m)S_1 - \mu_2\|^2. \quad (9)$$

The efficiency of estimating the refractive index from the condition of minimum of the discrepancy functional $F_{ij}(m, \kappa)$ in the form of formula (9) depends on the degree of variability of the functional in the vicinity of the rigorous solution which can be estimated numerically for different opto-microphysical state of the atmosphere and is determined by the values of optical characteristics μ_i and scattering angles for which the measurements have been carried out.

4. Finite-difference approximation. When direct and inverse problems are solved for polydisperse characteristics of scattering in the form of formula (5) (or formula (6)) the complexity can appear associated with the derivatives of the form $\partial K(\cdot)/\partial r$ of the corresponding Mie efficiency factors entering into the integrand. Therefore it has become necessary to construct algorithms for calculating the derivatives $\partial K/\partial r$ with strong alternating oscillations and large amplitude differences. Evaluation of integrals of the functions with such properties is a nontrivial problem and requires the application of the special-purpose quadrature schemes. In the simplest case the quantization of the

problem can be performed based on the scheme presented below.

To this end, for a given n we define the grid nodes $r_j = R \cdot j/n$ with a uniform step $\Delta = R/n$ in which the distribution $S(r)$ is approximated by a piecewise-linear function (spline) according to the formula

$$S(r) = \sum_{j=1}^n S_j N_j(r), \tag{10}$$

where $S_j = S(r_j)$ ($S(0) = 0$). The base functions $N_j(r)$ have the form

$$N_j(r) = N_0 \left(\frac{r - r_j}{\Delta} \right), \quad j = 1, 2, \dots, n, \tag{11}$$

where

$$N_0(r) = \begin{cases} 1 - |r|, & r \leq 1 \\ 0, & r > 1. \end{cases}$$

In such an approximation a set of functions $S(r)$ transforms to a set of vectors S with nondecreasing components:

$$0 < S_1 \leq S_2 \leq \dots \leq S_n \leq C, \tag{12}$$

where C is the upper estimate of the total cross section of particles. Substituting Eq. (10) into Eq. (5), after transformations, we obtain a finite-difference analog for Eq. (5)

$$\sum_{j=1}^n Q_j(\theta) S_j = \mu_j(\theta), \tag{13}$$

where

$$Q_j(\theta) = \bar{K}_{j-1} - \bar{K}_j, \quad j = 1, \dots, n; \tag{14}$$

$$\bar{K}_j(\theta) = \Delta^{-1} \int_{r_j}^{r_{j+1}} K(\theta, r) dr, \quad j = 0, 1, \dots, n-1; \tag{15}$$

$$\bar{K}_n(\theta) = 0.$$

Functions $\bar{K}_j(\theta)$ ($j \neq n$) are the values of the kernel $K(\theta, r)$ averaged over the intervals $[r_j, r_{j+1}]$. It can be seen from relations (13)–(15) that in the above-considered finite-difference scheme it is not necessary to calculate integrals involving the derivatives $\partial K / \partial r$.

5. The results of numerical simulation. Let us consider some examples illustrating the efficiency of the foregoing method in the numerical experiment as applied to the estimate of the parameters m and κ from angular polarization measurements. The haze N from Ref. 2 with the refractive index $1.5 - i \cdot 0$, was chosen as a model microstructural distribution. The microstructural distributions $S(r)$ were reconstructed by inverting the components of the scattering matrix $\mu_1(\theta)$ prescribed on a discrete set of angles θ_i , where $i = 1, \dots, p$ and $p = 18$ uniformly distributed on the interval $[0, 180^\circ]$. The discrepancy functional (8) for Eq. (7) was minimized with a set of vectors S subject to constraints (12) by the conditional gradient method.⁴ The parameters (m, κ) were estimated by minimizing the discrepancy functional

$F_{1k}(m, \kappa)$ in the form of formula (9) for the rest of the components of the scattering matrix $\mu_k(\theta)$, where $k = 2, 3, 4$, at the same scattering angles.

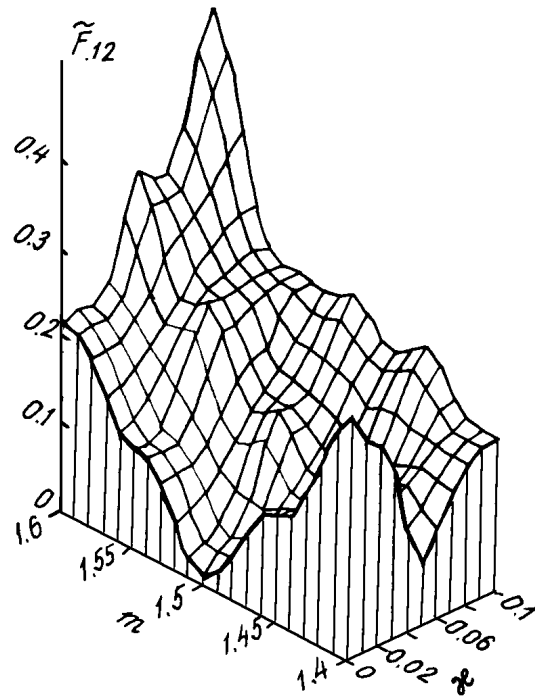


FIG. 1. A plot of the discrepancy functional $\tilde{F}_{12} = \|Q_2 S_1 - \mu_2\| / \|\mu_2\|$ vs the refractive index $m - i\kappa$ obtained in the numerical experiment for the model haze H ($m_0 = 1.5$ and $\kappa_0 = 0$).

The results of numerical experiments are shown in Figs. 1–3. Shown in Fig. 1 is the surface of the functional $\tilde{F}_{12}(m, \kappa) = F_{12}(m, \kappa) / \|\mu_2\|$ in space of the parameters (m, κ) in the vicinity of the rigorous solution ($m_0 = 1.5$ and $\kappa_0 = 0$). As can be seen from Fig. 1, in the considered region of variations in the parameters (m, κ) the surface $F_{12}(m, \kappa)$ has a quite complicated multi-extremum structure with global minimum at the point (m_0, κ_0) . If a real part of the refractive index m varies within the limits $[1.4, 1.6]$, then the range of relative variability of the functional $F_{12}(m, \kappa)$ about the norm $\|\mu_2\|$ lies within 28% for the exact value of the imaginary part $\kappa = \kappa_0$ and exceeds 50% for the deviation of κ as great as 0.1.

Since in the vicinity of the point of minimum (m_0, κ_0) the behavior of the functional $F_{12}(m, \kappa)$ is primarily determined by a noise component of the measured polarization characteristics, a set P_δ of points (m, κ) satisfying the inequality $F_{12}(m, \kappa) \leq \delta$, where δ depends on the error in assigning the functions μ_1 and μ_2 , can be considered as admissible solutions. The behavior of the functional $F_{12}(m, \kappa)$ in the vicinity of the point (m_0, κ_0) testifies to the fact that the errors in estimating one of the parameters, e.g., κ , results in errors in determining another parameter m when $F_{12}(m, \kappa)$ is minimized. In the case at hand such a mutual effect of errors becomes important for

$\Delta\kappa > 0.02$ and gives an error Δm in estimating the parameters m by minimizing $F_{12}(m)$ given that Δm was 0.05 for an *a priori* error $\Delta\kappa = 0.05$. The relation between the errors Δm and $\Delta\kappa$ determines a region of uncertainty in estimating the parameters m and κ by minimizing the functional $F_{12}(m, \kappa)$.

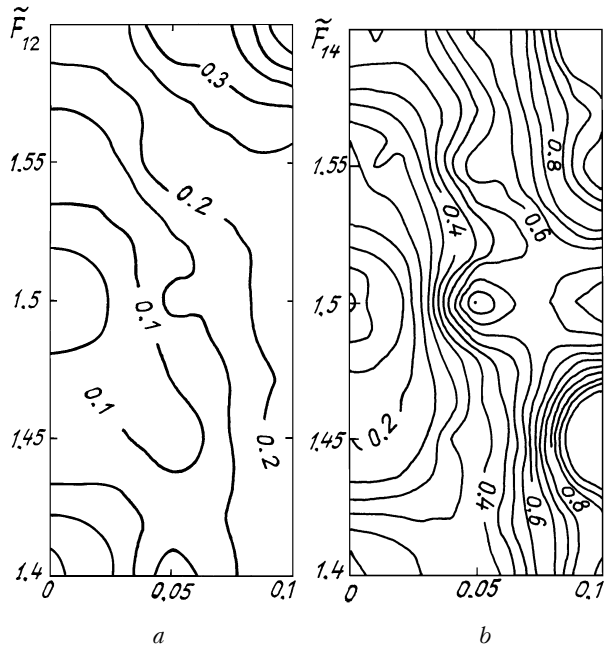


FIG. 2. Charts of contour lines of the discrepancy functionals \tilde{F}_{12} (a) and \tilde{F}_{14} (b) in the plane of the parameters (m, κ) ; the step of the contour lines is 0.05.

The regions of uncertainty when estimating the parameters m and κ can be found from Fig. 2a in which a chart of contour lines of the functional surface $F_{12}(m, \kappa)$ is shown. The contour lines in Fig. 2a define the boundaries of the region P_δ for different values δ . It is clear that the steeper the slopes of the surface $F_{12}(m, \kappa)$, the higher is the density of contour lines and the higher is the sensitivity of the functional $F_{12}(m, \kappa)$ to variations in the parameters being reconstructed.

For comparison, Fig. 2b shows a chart of contour lines of the functional $\tilde{F}_{14}(m, \kappa) = F_{14}(m, \kappa)/|\mu_4|$. In the vicinity of the point (m_0, κ_0) under consideration the variations of the functional $F_{14}(m, \kappa)$ are stronger than those of the functional $\tilde{F}_{12}(m, \kappa)$ and exceed 120%. Comparison of Figs. 2a and 2b reveals that with an equal step of contour lines (0.05) the line density is higher than that for the functional $\tilde{F}_{14}(m, \kappa)$. In this case, the region P_δ of admissible values of the parameters (m, κ) corresponding to a fixed level of discrepancy δ , e.g., $\delta = 10\%$, is much smaller for the functional $\tilde{F}_{14}(m, \kappa)$ than an analogous region bounded by the contour line of the same level of discrepancy for the functional $\tilde{F}_{12}(m, \kappa)$. This is

indicative of higher level of information content of a pair of polarization characteristics $\{\mu_1, \mu_4\}$ in comparison with the pair $\{\mu_1, \mu_2\}$ for the problem of reconstructing the refractive index $m - i\kappa$.

The analogous calculations were also made for a pair of characteristics $\{\mu_1, \mu_3\}$ which showed that a combination of such measurements is less sensitive to variations in the parameters being reconstructed compared to the aforementioned pairs of characteristics $\{\mu_1, \mu_2\}$ and $\{\mu_1, \mu_4\}$. To compare the information content of the three functionals $F_{1j}(m, \kappa)$ ($j = 2, 3, 4$) relative to the parameters being reconstructed, Fig. 3 shows their dependences on each of the parameters m and κ with an exact value of another parameter. The behavior of the functionals $F_{1j}(m, \kappa)$ ($j = 2, 3, 4$) shown in Fig. 3 is analogous to the dependences of discrepancy functionals derived in Ref. 6 based on the other calculational scheme.

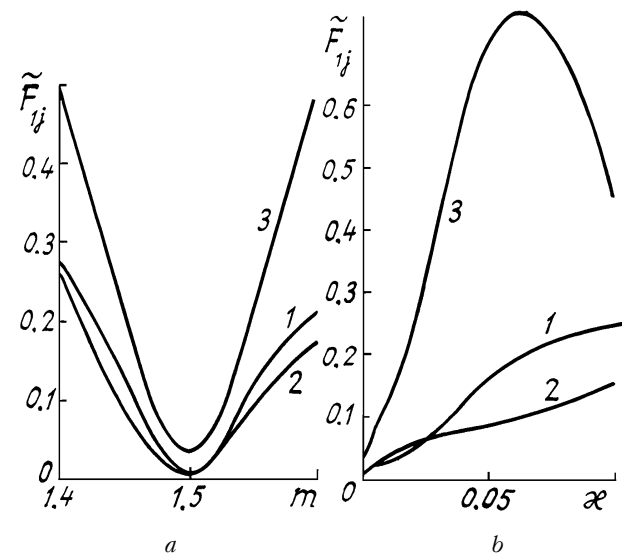


FIG. 3. A plot of the discrepancy functionals $\tilde{F}_{1j}(m, \kappa)$ ($j = 2, 3, 4$, curves 1–3) vs a real m (a) and imaginary κ (b) parts of the refractive index.

6. An example of interpreting the results of field experiments. In conclusion, let us consider an example of interpreting the polarization scattering phase functions of a coastal marine haze using the foregoing method. The polarization scattering phase functions were assigned in the form of a single-parameter model⁷ which described their transformation under conditions of variable turbidity of the atmosphere by means of an input parameter, i.e., the meteorological visibility range S_m . The results of reconstructing a real part of the refractive index m by inverting the model of polarization scattering phase functions depending on the aerosol extinction coefficient at the wavelength $\lambda = 0.55 \mu\text{m}$ are shown in Fig. 4a (curve 1). The vertical lines denote a margin of the refractive index m corresponding to a margin of 10% of the functional $\tilde{F}_{12}(m)$.

The data derived in Ref. 8 from the model of polarization scattering phase functions by the regularization method are shown here too for comparison (curve 2). The discrepancy in the estimates of m obtained by the two methods did not exceed 0.01.

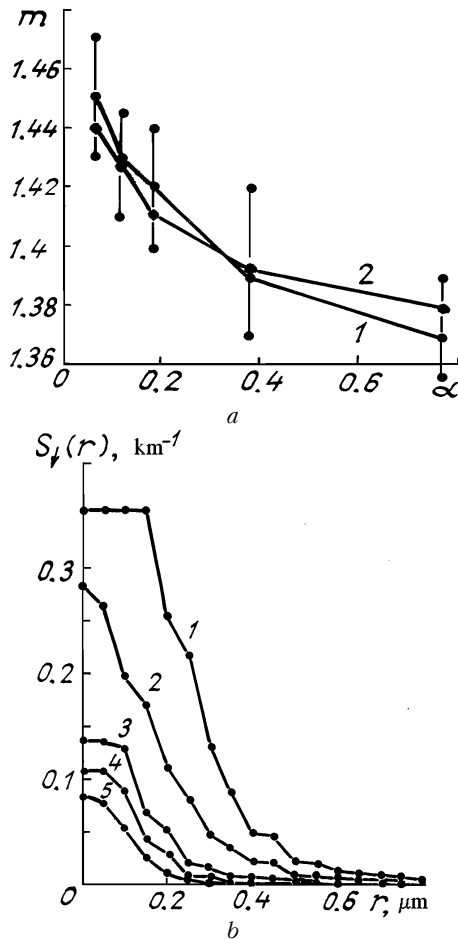


FIG. 4. An example of interpreting the model of polarization scattering phase functions for a coastal marine haze.⁷ a) Results of reconstructing a real part of the refractive index m as a function of the aerosol scattering coefficient α (0.55): curve 1 is obtained by the method described in the paper and curve 2 is obtained by the regularization method⁸ and b) a family of aerosol distributions $S_d(r)$ reconstructed for the meteorological visibility range $S_m = 5$ (curve 1), 10 (2), 20 (3), 30 (4), and 50 (5) km.

A family of aerosol distributions $S_d(r)$ corresponds to the reconstructed values of the refractive index m shown in Fig. 4b by the discrete counts $S_{d_j} - S_d(r_j)$ with the step $\Delta = 0.05 \mu\text{m}$. When the discrepancy function $F(8)$ was minimized, the *a priori* upper limit C subject to constraints (12) was fixed and equal to 0.4 km^{-1} for all of the chosen values S_m . A set of the values $S_d(r)$ at zero point characterizes the variability of the total geometric cross section of haze particles attendant to changes in the meteorological

visibility range S_m . Depicted in Fig. 4b are the data which enable us to determine, in a rather simple way, the transformation of the volume fill factor V as a function of the atmospheric turbidity (see Table I, the second row). The third row of Table I presents the results of calculation of V from the differential distributions $S(r)$ taken from Ref. 8. The discrepancy in the values of the volume fill factor V derived by two different methods are within 10%.

TABLE I. Results of reconstruction of the volume fill factors V for the coastal marine haze from the model of polarization scattering phase functions published in Ref. 7.

$S_m, \text{ km}^{-1}$	5	10	20	30	50
$V \cdot 10^{10}$	1.55	0.773	0.372	0.258	0.160
V from Ref. 8	1.31	0.705	0.386	0.257	0.158

Conclusion. Thus, a new numerical scheme for reconstructing the microstructure and the refractive index of aerosol particles from angular measurements of scattering matrix components has been proposed in this paper. The inversion method is based on the use of the integral aerosol particle size distributions and on the representation of the polydisperse scattering characteristics in the form of the Stieltjes integrals. Advantages of this approach include the fact that for such a statement a set of correctness incorporates a wider class of functions describing the aerosol particle size distributions. Moreover, when solving this problem it is unnecessary to choose the regularization parameter for the inverse problem with the approximately assigned operator. The given results of numerical modeling of the inverse problem for the components of the scattering matrix and the analysis of the information content of polarization measurements as well as the examples of reconstructing the microphysical parameters of aerosol from the field measurements completely agree with the results obtained by the other methods.

REFERENCES

1. I.E. Naats, *The Method of Inverse Problem in Atmospheric Optics* (Nauka, Novosibirsk, 1986), 199 pp.
2. D. Deirmendjian, *Electromagnetic Scattering on Spherical Polydispersions* (American Elsevier, New York, 1969).
3. A.N. Kolmogorov and S.V. Fomin, *Elements of the Theory of Functions and Functional Analysis* (Nauka, Moscow, 1968), 496 pp.
4. A.N. Tikhonov, A.V. Goncharkii, V.V. Stepanov, and A.G. Yagola, *Numerical Methods for Solving Ill-Posed Problems* (Nauka, Moscow, 1990), 230 pp.
5. V.E. Zuev and I.E. Naats, *Inverse Problems of Lidar Sensing of the Atmosphere* (Springer Verlag, New York, 1982).
6. V.V. Veretennikov, I.E. Naats, M.V. Panchenko, and V.Ya. Fadeev, *Izv. Akad. Nauk SSSR, Ser. FAO* **14**, No. 12, 1313–1317 (1978).
7. M.V. Kabanov, M.V. Panchenko, Yu.A. Pkhalagov, et al., *Optical Properties of Coastal Marine Hazes* (Nauka, Novosibirsk, 1988), 201 pp.
8. V.V. Veretennikov, M.V. Kabanov, and M.V. Panchenko, *Izv. Akad. Nauk SSSR, Ser. FAO* **22**, No. 10, 1042–1049 (1988).